Bounds to binding energies from the concavity of thermodynamical functions

B. K. Jennings
jennings@triumf.ca, TRIUMF, Vancouver BC, V6T2A3, Canada
B. R. Barrett
bbarrett@physics.arizona.edu, Department of Physics,
University of Arizona, Tucson, AZ 85721, USA
B. G. Giraud
bertrand.giraud@cea.fr, Service de Physique Théorique,
DSM, CE Saclay, F-91191 Gif/Yvette, France
(Dated: February 1, 2008)

Sequences of experimental ground-state energies are mapped onto concave patterns cured from convexities due to pairing and/or shell effects. The same patterns, completed by a list of excitation energies, can be used to give numerical estimates of the grand potential $\Omega(\beta,\mu)$ for a mixture of nuclei at low or moderate temperatures $T=\beta^{-1}$ and at many chemical potentials μ. The average nucleon number $\langle\mathbf{A}\rangle(\beta,\mu)$ then becomes a continuous variable, allowing extrapolations towards nuclear masses closer to drip lines. We study the possible concavity of several thermodynamical functions, such as the free energy and the average energy, as functions of $\langle\mathbf{A}\rangle$. Concavity, when present in such functions, allows trivial interpolations and extrapolations providing upper and lower bounds, respectively, to binding energies. Such bounds define an error bar for the prediction of binding energies. An extrapolation scheme for such concave functions is tested. We conclude with numerical estimates of the binding energies of a few nuclei closer to drip lines.

I. INTRODUCTION

The observation of a valley of stability and the search for mass formulae belong to the oldest subjects studied in nuclear physics. Given the neutron and proton numbers N and Z as independent variables and the corresponding atomic number, $A\equiv N+Z$, terms such as volume energy $\propto(N+Z)$, surface tension $\propto(N+Z)^{\frac{2}{3}}$, Coulomb energy $\propto Z(Z-1)/(N+Z)^{1/3}$, symmetry energy $\propto(N-Z)^2/(N+Z)$, etc. flourish in the literature, and a great deal of attention has been dedicated to the consideration of finer corrections, such as, for instance, terms $s(N,Z)$ and $p(N,Z)$ that account for shell and pairing effects, respectively. This work is motivated by the observation that the dominant terms, namely $\propto(N+Z)$, $\propto Z(Z-1)$ and $\propto(N-Z)^2$, define a paraboloid energy surface, notoriously *concave*.

Upper and lower bounds to nuclear binding energies can be deduced from such a concavity, provided that deviations from concavity, possibly induced by subdominant terms like $\propto(N+Z)^{\frac{2}{3}}$, $s(N,Z)$, $p(N,Z)$, etc., can be corrected. In a previous article [1], we showed how elementary transformations of data could generate truly concave patterns. This was obtained by an analysis of the table of second differences between binding energies, then by a removal of pairing energy, and finally by an *ad hoc*, but minimal, parabolic term added to nuclear energies, if necessary.

Concavity is also a property of several thermodynamical functions. An extension of the analysis at zero temperature [1] to a finite temperature theory is in order. This extension is the main subject of the present paper. For the sake of simplicity this paper, like [1], considers only sequences of isotopes and, thus, takes advantage of concavity with respect to N only; Z is frozen. A generalization to concavity with respect to both N and Z is left to future work.

In Sec. II we briefly recall the method, explained in [1], for the tuning of actual experimental data into concave patterns. In Sec. III we discuss properties of that grand potential, $\Omega(\beta,\mu)$, which can be deduced from the experimental data after their tuning. Other thermodynamical functions will also be considered, and their concavity will be tested. Bounds will be found, and an error bar for predictions will be estimated. Section IV contains a brief discussion of the problems raised by extrapolations of concave functions. A discussion and conclusion are given in Sec. V.

II. CONCAVITY WITH EXPERIMENTAL GROUND-STATE ENERGIES

Our argument is illustrated numerically, by using a sequence of isotopic ground-state binding energies, $-E_A$. Consider the table from ^{110}Sn to ^{137}Sn, studied in [1] at zero temperature, because we later want to extend it at finite temperature by including the energies of excited states. It reads, in keV,
{934562, 942743, 953529, 961272, 971571, 979117, 988680, 995625, 1004952, 1011437. 1020544, 1026715, 1035529, 1041475, 1049962, 1055695, 1063889, 1069448, 1077348, 1082713, 1090400, 1095615, 1102917, 1105335, 1109075, 1111310, 1115087, 1117150}.

It should be noted that such data come from Refs. [2, 3, 4, 5]. These sources often quote the binding energy per nucleon instead of the total binding energy itself and such values per nucleon are given to varying numbers of significant figures, from four to seven. Consequently, even though we quote and use all our binding energies to six or seven significant figures, for consistency reasons and for ease of performing our calculations, our values are generally accurate only to the order of tens of keV. It must be understood that all energies stated in this paper are in units of keV.

Despite a well known linear trend because of a "not too much fluctuating average energy per nucleon", this list of energies is far from making a smooth pattern. It is even less of a concave one. The sequence of 26 second differences (SDs), $E_{A+1} - 2E_A + E_{A-1}$,
{-2606, 3043, -2556, 2753, -2018, 2619, -2382, 2841, -2622, 2937, -2643, 2868, -2542, 2755, -2460, 2634, -2341, 2535, -2322, 2473, -2088, 4885, -1323, 1506, -1542, 1714},
gives estimates of the "curvatures" of the pattern. It is far from containing only positive numbers. On the contrary, its signs alternate, systematically. The wiggling between SD's centered at odd and even nuclei (or staggering) has, roughly speaking, a constant amplitude. (Notice, however, the maximum SD, 4885, due to the shell closure at ^{132}Sn, and the weakening of the numbers beyond ^{132}Sn.)

These alternating signs are obviously due to the gains of binding for even Sn nuclei because of pairing. Add to each *even* nucleus energy a fixed number, for example $p(N, Z) = 1050$ keV, to suppress the increase of binding due to pairing. The resulting list of SDs is attenuated by an amount equal to $\pm 2p$ and now reads,
{-506, 943, -456, 653, 82, 519, -282, 741, -522, 837, -543, 768, -442, 655, -360, 534, -241, 435, -222, 373, 12, 2785, 777, -594, 558, -386}.
All numbers are now significantly smaller than their partners in the previous list of SD's, except for the "spike" at ^{132}Sn. The latter is positive, and, hence causes no deviation from concavity. The interesting point is the most negative number in the list, namely -594 keV. All negative curvatures can be converted into positive ones if we add to every energy an artificial, parabolic correction, which was chosen in [1] as, $P \times (A - 118)^2$, with $P = 300$ keV. Incidentally, the lowest point of the parabola is arbitrary, because SDs will increase by just a constant, namely twice the coefficient P of the A^2 term.

Hence, after such a 600 keV shift, the previous sequence of SDs becomes entirely positive,
{94, 1543, 144, 1253, 682, 1119, 318, 1341, 78, 1437, 57, 1368, 158, 1255, 240, 1134, 359, 1035, 378, 973, 612, 3385, 1377, 6, 1158, 214},

In short, a "concavity ensuring" manipulation for the Sn isotope energies consists in replacing each energy E_A by $E'_A = E_A + 1050 \times Mod[A + 1, 2] + 300 \times (A - 118)^2$. This indeed creates a concave pattern. The list of such tuned energies, $-E'_A$, reads,
{914312, 928043, 941679, 953772, 965721, 976417, 986430, 995325, 1003902, 1011137, 1018294, 1024015, 1029679, 1033975, 1038112, 1040995, 1043639, 1045148, 1046298, 1046413, 1046150, 1044915, 1043067, 1037835, 1031225, 1024610, 1016837, 1008850}.
The choice of the two parameters, p=1050 keV and P=300 keV, is empirical: one must find a pairing correction leading to a minimal parabolic correction inducing concavity. Other choices for $\{p, P\}$ are obviously possible. Anyhow, such parameters must be readjusted for different regions of the table of nuclei.

When concavity is obtained, it is trivial to see that extrapolations from two points on the concave pattern allow predictions of lower bounds to nuclear energies. In the same way, it is trivial that interpolations provide upper bounds. Then, from such bounds for energies E', one recovers bounds, of strictly the same quality, for the physical energies E. This is obtained by subtracting from E' bounds their "tuning terms".

In [1] we showed that the quality of such bounds is indeed good, and that interpolations and extrapolations from the raw, non concave pattern, are less satisfactory. But there is a more profound reason why a concave pattern is necessary. Indeed, several thermodynamical functions, governed by theorems proving their concavity, have a notoriously singular limit at zero temperature: they become non analytical and are just piecewise continuous. Their limit plots are made of segments; derivatives are discontinuous at turning points. Because of the staggering effect, the *concave envelope* of the raw pattern of E_A would contain only the even isotopes. Concavity is thus necessary for a theory which must accommodate both odd and even nuclei. The thermodynamical functions studied in the next section, Sec. III, therefore, preferably use concave energies E'_A and the corresponding excited state energies E'_{nA}.

III. CONCAVITY WITH THERMODYNAMICAL FUNCTIONS

Consider the particle number operator $\mathbf{A}$ and a familiar nuclear Hamiltonian $\mathbf{H} = \sum_{i=1}^{A} t_i + \sum_{i>j=1}^{A} v_{ij}$, where A, t and v are the mass number, one-body kinetic energy and two-body interaction, respectively. Nuclear data tables give precise values for a large number of lowest lying eigenvalues E_{nA} of $\mathbf{H}$, for many nuclei. One may thus reasonably

estimate the grand partition function,

$$\mathcal{Z}(\mu,\beta) = \mathrm{Tr}\, \exp\left[\beta\left(\mu\mathbf{A}-\mathbf{H}\right)\right] = \sum_{nA}(2j_{nA}+1)\exp\left[\beta\left(\mu A - E_{nA}\right)\right], \tag{1}$$

provided that i) the temperature, $T=\beta^{-1}$, is low enough to allow a truncation of the spectrum to include only those states provided by the tables and ii) the chemical potential, μ, selects mainly those nuclei in which we are interested. Let $\langle\ \rangle$ denote, as usual, a statistical average. The (equilibrium!) density operator in Fock space, $\rho = \mathcal{Z}^{-1}\exp\left[\beta\left(\mu\mathbf{A}-\mathbf{H}\right)\right]$, ensures that the following grand potential, $\Omega(\mu,\beta) = \langle\left(\mu\mathbf{A}-\mathbf{H}\right)\rangle + T\,S$, is maximum in the space of many-body density matrices with unit trace, since, by definition, $\langle\mathbf{A}\rangle = \mathrm{Tr}\,\rho\,\mathbf{A}$, $\langle\mathbf{H}\rangle = \mathrm{Tr}\,\rho\,\mathbf{H}$, with the entropy, $S=-\mathrm{Tr}\left(\rho\,\log\rho\right)$. Our use of a slightly non-traditional Ω makes the upcoming proofs of concavity somewhat easier. This grand potential also reads,

$$\Omega(\mu,\beta) = \beta^{-1}\ln\,\mathcal{Z} = \beta^{-1}\ln\left\{\sum_{nA}(2j_{nA}+1)\exp\left[\beta\left(\mu A - E_{nA}\right)\right]\right\}, \tag{2}$$

Trivial manipulations then give the relevant statistical averages $\langle\ \rangle$ of particle numbers and energies, together with their derivatives and fluctuations,

$$\partial\Omega/\partial\mu = \langle\mathbf{A}\rangle = \sum_A A\ p_A, \quad p_A = \mathcal{Z}^{-1}\sum_n(2j_{nA}+1)\exp\left[\beta\left(\mu A - E_{nA}\right)\right], \tag{3}$$

and

$$\partial^2\Omega/\partial\mu^2 = \partial\langle\mathbf{A}\rangle/\partial\mu = \beta\,\left(\,\langle\mathbf{A}^2\rangle - \langle\mathbf{A}\rangle^2\,\right), \tag{4}$$

then

$$\partial\Omega/\partial T = S = \ln\mathcal{Z} - \beta\,\langle\left(\mu\mathbf{A}-\mathbf{H}\right)\rangle, \tag{5}$$

or as well,

$$\langle\mathbf{H}\rangle = \mathcal{Z}^{-1}\sum_{nA}(2j_{nA}+1)E_{nA}\,\exp\left[\beta\left(\mu A - E_{nA}\right)\right]. \tag{6}$$

Furthermore,

$$\partial^2\Omega/\partial T^2 = \beta^3\left[\langle\left(\mu\mathbf{A}-\mathbf{H}\right)^2\rangle - \langle\left(\mu\mathbf{A}-\mathbf{H}\right)\rangle^2\right], \tag{7}$$

and

$$\partial^2\Omega/(\partial\mu\,\partial T) = -\beta^2\left[\langle\,\mathbf{A}\left(\mu\mathbf{A}-\mathbf{H}\right)\rangle - \langle\mathbf{A}\rangle\,\langle\left(\mu\mathbf{A}-\mathbf{H}\right)\rangle\right]. \tag{8}$$

Since the values of A are integers, all such functions $\mathcal{Z},\Omega,...,\langle\mathbf{H}\rangle,...$ are clearly periodic functions of μ, with a purely imaginary period, $2\pi i/\beta$. This is of interest for the study of holomorphy domains with respect to both μ and β, but we will freeze β as real in the following and consider functions of a real μ.

Consider the (symmetric!) matrix of second derivatives,

$$\mathcal{D} = \begin{bmatrix} \partial^2\Omega/\partial\mu^2 & \partial^2\Omega/(\partial\mu\,\partial T) \\ \partial^2\Omega/(\partial T\,\partial\mu) & \partial^2\Omega/\partial T^2 \end{bmatrix}. \tag{9}$$

Its trace is obviously positive. Now, with short notations, $\mathbf{B}$, $\Delta\mathbf{A}$ and $\Delta\mathbf{B}$ for $\mu\mathbf{A}-\mathbf{H}$, $\mathbf{A}-\langle\mathbf{A}\rangle$ and $\mathbf{B}-\langle\mathbf{B}\rangle$, respectively, its determinant reads,

$$\det\mathcal{D} = \beta^4\ \det\begin{bmatrix} \langle\left(\Delta\mathbf{A}\right)^2\rangle & -\langle\left(\Delta\mathbf{A}\right)\left(\Delta\mathbf{B}\right)\rangle \\ -\langle\left(\Delta\mathbf{A}\right)\left(\Delta\mathbf{B}\right)\rangle & \langle\left(\Delta\mathbf{B}\right)^2\rangle \end{bmatrix}. \tag{10}$$

A trivial use of Schwarz's inequality shows that $\det\mathcal{D}$ is positive. Thus, $\mathcal{D}$ is a positive definite matrix. In other terms, Ω is a concave function of μ and T. In turn, the double Legendre transform, with respect to both μ and T,

$$\mu\ \partial\Omega/\partial\mu + T\,\partial\Omega/\partial T - \Omega = \langle\mathbf{H}\rangle, \tag{11}$$

shows that $\langle \mathbf{H} \rangle$ is a concave function of both $\langle \mathbf{A} \rangle$ and S, the conjugate variables of μ and T, respectively.

In the following, we do not perform the full, double Legendre transform. We rather retain an intermediate representation, with $\langle \mathbf{A} \rangle$ and either T or β. We stay with real variables and functions. We can stress that, while $\mathbf{A}$ has a discrete spectrum, conversely $\langle \mathbf{A} \rangle$ is continuous, a monotonically increasing function of μ, smooth provided β is finite. The monotonicity results from Eq. (4). Actually, at low temperatures, strong derivatives signal the onset of discrete jumps due to the integer spectrum of $\mathbf{A}$, but we may stay away from this "jumpy" regime in the following, temporarily at least. Anyhow, at any fixed, finite β, the smoothness and monotonicity of $\langle \mathbf{A} \rangle$ with respect to μ allows a reasonably easy numerical calculation of the inverse function $\mu\left(\langle \mathbf{A} \rangle\right)$. A main argument of this section is thus, at fixed temperatures, to use $\langle \mathbf{A} \rangle$ as a continuous variable and attempt extrapolations towards unknown nuclei.

For this, given a fixed value of T, we keep track of $\langle \mathbf{A} \rangle$ and $\langle \mathbf{H} \rangle$ as functions of μ. Since the functional inversion from $\langle \mathbf{A} \rangle(\mu)$ to $\mu(\langle \mathbf{A} \rangle)$ is reasonably easy, we plot $\langle \mathbf{H} \rangle$ in terms of $\langle \mathbf{A} \rangle$ and can attempt an extrapolation for further values of $\langle \mathbf{A} \rangle$. This extrapolation can be considered as a candidate for a mass formula, at that finite temperature T.

According to Eq. (7), the average, constrained energy, $\langle (\mathbf{H} - \mu \mathbf{A}) \rangle$, is a monotonically decreasing function of β. Furthermore, for negative chemical potentials μ at least, and more generally if A has an upper bound, the operator, $\mathbf{H} - \mu \mathbf{A}$, is bounded from below. Therefore there is a convergence of the process consisting in i) extrapolating with respect to μ both $\langle (\mathbf{H} - \mu \mathbf{A}) \rangle$ and $\langle \mathbf{A} \rangle$ for fixed values of β, then ii) eliminating μ to generate the β-parametrized "mass formula" $\langle \mathbf{H} \rangle \left(\langle \mathbf{A} \rangle, \beta \right)$, and finally iii) considering the limit of this mass formula when $\beta \to +\infty$. Alternately, it is equivalent, and maybe more efficient, to first eliminate μ and then extrapolate the "mass formula" $\langle \mathbf{H} \rangle \left(\langle \mathbf{A} \rangle, \beta \right)$, first with respect to $\langle \mathbf{A} \rangle$, then with respect to β.

Are there concavity properties in this intermediate representation? Clearly, a simple Legendre transform of Ω, with respect to μ only, returns a free energy, $\langle \mathbf{H} \rangle - T\,S$, as a concave function of $\langle \mathbf{A} \rangle$ and T. If T is low enough to allow the product $T\,S$ to be neglected, then, at fixed T, one may accept that $\langle \mathbf{H} \rangle$ is an "almost" concave function of $\langle \mathbf{A} \rangle$. This assumption will be tested by the numerical results which follow. Incidentally, a straightforward calculation yields,

$$\frac{\partial^2 \langle \mathbf{H} \rangle}{\partial \langle \mathbf{A} \rangle^2} \left(\langle \mathbf{A} \rangle, \beta \right) \propto \left(\langle \mathbf{A}^2 \rangle - \langle \mathbf{A} \rangle^2 \right) \langle \mathbf{A}^2 \mathbf{H} \rangle + \left(\langle \mathbf{A} \rangle \langle \mathbf{A}^2 \rangle - \langle \mathbf{A}^3 \rangle \right) \langle \mathbf{A} \mathbf{H} \rangle + \left(\langle \mathbf{A} \rangle \langle \mathbf{A}^3 \rangle - \langle \mathbf{A}^2 \rangle^2 \right) \langle \mathbf{H} \rangle, \tag{12}$$

with a positive factor, $\left(\langle \mathbf{A}^2 \rangle - \langle \mathbf{A} \rangle^2 \right)^{-3}$. This simplifies into

$$\frac{\partial^2 \langle \mathbf{H} \rangle}{\partial \langle \mathbf{A} \rangle^2} \left(\langle \mathbf{A} \rangle, \beta \right) \propto \langle \, (\Delta \mathbf{A})^2 \, \rangle \, \langle \, (\Delta \mathbf{A})^2 \, \Delta \mathbf{H} \, \rangle - \langle \, (\Delta \mathbf{A})^3 \, \rangle \, \langle \, \Delta \mathbf{A} \, \Delta \mathbf{H} \, \rangle, \tag{13}$$

if one uses the already defined, centered operator $\Delta \mathbf{A}$ and the similarly centered operator $\Delta \mathbf{H} = \mathbf{H} - \langle \mathbf{H} \rangle$. From Eqs. (12,13), concavity is unclear; we shall have to test it numerically.

The results, which follow, use [6] and also the tables, already quoted [2, 3, 4, 5]. Using the first 10 levels of ^{110}Sn to ^{137}Sn, successively, and fewer levels if less than 10 are known, we calculate $\mathcal{Z}$, see Eq. (1). For those rare cases where the spin j_{nA} is ambiguous we choose the lowest of the suggested spins. If the spin is completely unknown, we set it to be either 0 or 1/2, according to A. These tactics minimize the statistical influence of such rare cases. For a future independent treatment of the proton and neutron numbers, we actually use a neutron number operator $\mathbf{N} = \mathbf{A} - 50$ rather than $\mathbf{A}$ in Eqs. (1)-(12); our chemical potential μ is truly for neutrons. However, for easier reading, the upcoming plots use $\langle \mathbf{A} \rangle = \langle \mathbf{N} \rangle + 50$.

The lower and upper curves in the left part of Fig. 1 are the plots of the function $\langle \mathbf{H} \rangle (\langle \mathbf{A} \rangle)$ when $T = 20$ keV and $T = 2$ MeV, respectively. The increase of $\langle \mathbf{H} \rangle$ when T increases is transparent. Note, however, that a lack of excited states in our data base beyond ^{132}Sn weakens this temperature effect. Also striking is the apparent concavity of both curves. It is found that the lower temperature, 20 keV, is low enough to allow $\langle \mathbf{H} \rangle$ to run, in practice, through all the experimental energies for the *even* nuclei; the function follows the *concave envelope* of the experimental pattern. For graphical convenience, Fig. 1 shows the plots for $124.7 \leq \langle \mathbf{A} \rangle \leq 135.3$ only, but the same observations hold for full plots, with $110 \leq \langle \mathbf{A} \rangle \leq 137$. As a test, we also calculated $\langle \mathbf{H} \rangle$ when the levels of ^{132}Sn are omitted from the trace sum, Eq. (1), see the right part of Fig. 1, where now the concave envelope goes through the dots representing two odd nuclei, ^{131}Sn and ^{133}Sn, and ignores the dot representing ^{132}Sn. Similar verifications of other concave envelopes were obtained by removing other nuclei when calculating $\mathcal{Z}$.

Then Fig. 2 shows what happens when one calculates a tuned partition function, $\mathcal{Z}'$, and all resulting functions S', $\langle \mathbf{A} \rangle'$, $\langle \mathbf{H} \rangle'$, etc. by using concave tuned energies, $E'_{nA} = E_{nA} + 1050 \times Mod[A+1, 2] + 300 \times (A - 118)^2$. The dots in Fig. 2 now represent ground-state tuned energies; hence, concave envelopes do not eliminate odd nuclei. Now both even and odd nuclei can be accounted for by the function $\langle \mathbf{H} \rangle'$, except, as shown by the right part of Fig. 2, for those nuclei which have been voluntarily omitted from the trace, Eq. (1).

To verify whether concave envelopes and concavity result from negligible values of the entropy term in the free energy, or, more precisely, negligible values of its second derivative, a calculation of $T\,S$, for bare data, and of its partner $T\,S'$, for tuned data, is in order. Figure 3 shows decimal log plots of the ratio, $|\,T\,S'/\langle \mathbf{H} \rangle'\,|$, as a function

of $\langle \mathbf{A} \rangle$, for $T = 100$, 300 and 2000 keV, respectively. At the higher temperature, 2 MeV, an approximately constant ratio is observed, except for edge effects at both ends of our data base. The almost constant ratio favors concavity. Moreover, the ratio typically does not exceed 10^{-2}. This is small, but might not be small enough, because then $T\,S'$ remains close to 10 MeV, the order of magnitude of $|E_{A+1} - E_A|$, a first difference and a binding energy per nucleon. For $T = 300$ keV, the ratio becomes smaller, $\sim 10^{-3}$ or less, but it acquires some structure, because of the low level density of ^{132}Sn in particular. Again lower ratios, smaller than 4×10^{-4}, are found for $T = 100$ keV, but now with strong variations. It is clear that odd nuclei, because of their higher level density due to the absence of a pairing gap in their spectra, induce maxima. As a consequence of such strong variations, translating into strong first and second derivatives, it is not excluded that SDs coming from $T\,S'$ might prevent $\langle \mathbf{H} \rangle'$ from having the concavity property of the free energy, $\langle \mathbf{H} \rangle' - T\,S'$. Obviously, the same difficulty might arise with $\langle \mathbf{H} \rangle$ and its concave envelopes. We must therefore numerically calculate second derivatives, see Eqs. (12,13).

The left part of Fig. 4 shows plots of the right-hand side of Eqs. (12,13), multiplied by $\left(\langle \mathbf{A}^2 \rangle' - \langle \mathbf{A} \rangle'^2\right)^{-2}$. This is for tuned data. The additional denominator, $\left(\langle \mathbf{A}^2 \rangle' - \langle \mathbf{A} \rangle'^2\right)$, is omitted for graphical reasons. The upper full line represents the situation when $T = 1$ MeV; the second derivative, $\partial^2 \langle \mathbf{H} \rangle' / \partial \langle \mathbf{A} \rangle'^2$, remains positive and does so until $T \sim 750$ keV, see the dashed line in the left-hand side of the figure. For lower temperatures, however, negative values appear. For instance, the lower full curve, corresponding to $T = 500$ keV, indicates small, but definitely negative values between ^{130}Sn and ^{131}Sn. Our numerical tests show that the occurrence of such negative, actually moderate, values for lower temperatures seems to be frequent, while not systematic. Furthermore, such "negativity accidents" turn out to be worse if we use untuned data, for the obvious reason that the untuned data lacked concavity in the first place.

A possible reason for the negativity accidents with tuned data might be that the fluctuation of $\mathbf{A}$ is not large enough to justify our use of $\langle \mathbf{A} \rangle'$ as a continuous variable. Since it interpolates between integers, a fluctuation of order ~ 1, or at least $\sim .5$, might be necessary. As shown by the three plots in the right part of Fig. 4, corresponding to $T = 1000$, 500 and 100 keV from the upper to the lower plots, respectively, a minimum temperature is needed to avoid too small a fluctuation of the particle number. Furthermore, the low level density in ^{132}Sn obviously reinforces a reduction of fluctuations and the small SDs obtained by us in the tuned pattern of ground-state energies allow localized deviations of concavity. The deviations are too weak to appear on Fig. 2, however.

At this stage, the situation can be summarized as follows. On the one hand, the tuned pattern of experimental energies shows concavity, but the concavity of $\langle \mathbf{H} \rangle'$ as a function of $\langle \mathbf{A} \rangle'$ is not sure, although it seems to occur most of the time. On the other hand, we have a theorem proving concavity for the free energy, either $\mathbf{F} \equiv \langle \mathbf{H} \rangle - T\,S = \mu\,\langle \mathbf{A} \rangle - \Omega$ or $\mathbf{F}' \equiv \langle \mathbf{H} \rangle' - T\,S' = \mu\,\langle \mathbf{A} \rangle' - \Omega'$, as functions of T and $\langle \mathbf{A} \rangle$ or $\langle \mathbf{A} \rangle'$, respectively. For instance, elementary derivations show that, in that representation where $\langle \mathbf{A} \rangle$ (or $\langle \mathbf{A} \rangle'$) and β are the primary variables,

$$\frac{\partial \mathbf{F}'}{\partial \beta} = \beta^{-2}\,S', \qquad \frac{\partial \mathbf{F}'}{\partial \langle \mathbf{A} \rangle'} = \mu \quad \text{and} \quad \frac{\partial^2 \mathbf{F}'}{\partial \langle \mathbf{A} \rangle'^2} = \frac{T}{\langle \mathbf{A}^2 \rangle' - \langle \mathbf{A} \rangle'^2}\,. \tag{14}$$

The removal of the entropy term, leading from the free energy to the energy, can destroy the concavity, somewhat weakly.

We are not much interested in $\mathbf{F}$, because, as stated earlier, its concavity skips odd nuclei. Thus, the remainder of this section will consider $\mathbf{F}'$, at fixed T, and we shall assume that T is low enough to make TS' small with respect to $\langle \mathbf{H} \rangle'$. This approximation can be verified later, in due time. Our rationale will be that $\langle \mathbf{H} \rangle'$, even though it might deviate from concavity, will stay close enough to the concave $\mathbf{F}'$. Their difference, TS', a positive quantity, will define an error bar between a lower bound $\mathbf{F}'$ and an upper bound $\langle \mathbf{H} \rangle'$ for ground-state energies.

Consider Fig. 5. The dots represent the ground-state tuned energies, the upper full curve is the plot of $\langle \mathbf{H} \rangle'(\langle \mathbf{A} \rangle')$ when $T = 1$ MeV, and the lower dashed curve is the plot of $\mathbf{F}'(\langle \mathbf{A} \rangle')$ at the same temperature. There is no need to stress that two such curves make a band defining upper and lower bounds for the experimental energies. Moreover, a similar, but narrower band is obtained if T decreases. The lower full curve and the upper dashed one in Fig. 5 represent $\langle \mathbf{H} \rangle'$ and $\mathbf{F}'$, respectively, for $T = 250$ keV. The following properties, i) the average energy and the free energy are increasing and decreasing, respectively, functions of T, ii) the energy is larger than the free energy and iii) the entropy term by which they differ vanishes when T vanishes, are not big surprises. It can be concluded that, in so far as thermodynamical functions can be calculated at low enough temperatures, precise "accuracy bands" may be available. Their, hopefully analytic, continuation for higher and/or lower values of A than those available in nuclear data tables provides a scheme making predictions for exotic nuclei.

An estimate of the entropy term is now useful. Given μ and a *large* β, let A_0 and E'_0 correspond to that nucleus whose ground-state energy maximizes the exponential, $\exp[\beta\,(\mu A - E'_{0A})]$. Consider now the first subdominant exponential. It might be generated by the first excited state of the same nucleus, or by the ground-state of one of its neighbors. Let A_1 and E'_1 be its parameters and define $\Delta = \mu\,(A_1 - A_0) - (E'_1 - E'_0)$. Concavity guarantees that $\Delta < 0$. Whenever β is large enough, it is trivial to reduce the grand canonical ensemble to a two state ensemble, and the entropy then

boils down to $s = -e^{\beta\,\Delta}\,\beta\,\Delta$. Hence, the product, $T\,s = -e^{\beta\,\Delta}\,\Delta$, vanishes exponentially fast when $\beta \to \infty$. The rate of decrease is governed by that scale defined by Δ, to be extracted from the tuned data. Then one can estimate an order of magnitude for the difference between the free energy and the energy. This estimate can be viewed as an error bar for the prediction of exotic nuclei via the present "concavity method".

IV. FURTHER VERIFICATION OF CONCAVITY PROPERTIES AND, THEN, EXTRAPOLATIONS

After our previous illustration with the Sn isotopes, we now calculate thermodynamical functions from a sequence of Sm isotopes, i.e. ^{135}Sm to ^{144}Sm. We want to again observe the behavior of such thermodynamical functions and, furthermore, extrapolate them. The extrapolation might provide "predictions" of the binding energies of lighter isotopes, from ^{128}Sm to ^{134}Sm for instance, which are quoted by the data tables [2]-[5]. According to the same data tables, indeed, the available accuracies for such lighter Sm nuclei still leave room for a large amount of theory.

Our list of raw data, $-E_A$, is, from ^{128}Sm to ^{144}Sm,
{1023616, 1034967, 1048320, 1059004, 1072104, 1082088, 1094512, 1103976, 1116005, 1125291, 1136834, 1145788, 1156935, 1165489, 1176615, 1185216, 1195736}.
We will not use the first seven nuclei in our calculations of $\langle \mathbf{A} \rangle'$, $\langle \mathbf{H} \rangle'$, $\mathbf{F}'$, etc., because of limited and/or poorly known data for those nuclei. The last ten data define eight SD's,
{2743, -2257, 2589, -2193, 2593, -2572, 2525, -1919}.
With a pairing correction parameter, $p = 1250$, and a parabolic correction parameter, $P = 36$, the SD's become
{315, 315, 161, 379, 165, 0, 97, 653}.
Finally our list of tuned energies,

$$E'_A = E_A + 10000 \times A - 245000 + 1250 \times Mod[A+1, 2] + 36 \times (A - 139)^2, \tag{15}$$

reads, {1600, 569, -147, -548, -788, -649, -345, -41, 360, 1414}.
The constant subtraction term, -245000, and the linear additive one, $10000 \times A$, are here just for graphical and numerical convenience; they do not change the SD's. The tuning process is illustrated by Fig. 6. In its left part, note the almost concave pattern made by the dots, the result of the pairing correction.
In the right part of Fig. 6, the dots represent tuned energies, see Eq. (15), from ^{132}Sm to ^{146}Sm, while the curve represents a least square fit, between only ^{135}Sm to ^{144}Sm, by a quadratic polynomial. The list of errors, $E'_{lsf}(A) - E'_A$, generated by this most simple fit from ^{135}Sm to ^{144}Sm, is, {-109, 46, 101, 58, 71, -79, -178, -61, 176, -24}. The right part of Fig. 6 shows that an extrapolation towards lighter nuclei can be considered. But an extrapolation towards heavier ones seems to be much less valid, with bad lower bounds.

The corresponding energies E'_{nA} of excited states [6], from ^{135}Sm to ^{144}Sm, are now used for the calculation of thermodynamical functions, Ω', $\langle \mathbf{A} \rangle'$, $\langle \mathbf{H} \rangle'$, etc. We take into account the lowest ten states per nucleus, whenever possible, and ambiguous spins are set to their minimum possible values. The result is shown in Fig. 7. It confirms all the analysis done with the Sn isotopes. The left part of Fig. 7 shows the fluctuations of $\langle \mathbf{A} \rangle'$ for $T = 200$ keV, (upper curve), and $T = 100$ keV, (lower curve), respectively. Except at both ends of the list of data used for the calculation, a fluctuation of at least $\sim .5$ is observed. This seems compatible with an extrapolation. Note, however, that difficulties are not excluded, because, indeed, the complete vanishing of the fluctuation at ^{135}Sm and ^{144}Sm is not a good omen.

Such end effects seem to be weaker in the right part of Fig. 7, which shows, again for the same temperatures, the behaviors of the average energy and the free energy. Dashed curves correspond to $T = 200$ keV and full curves to 100 keV, respectively. The curves above the dots represent $\langle \mathbf{H} \rangle'$ and those below them represent $\mathbf{F}'$. We, thus, see again "error bands", which shrink when T diminishes.

It is tempting to use the pair of curves, $\langle \mathbf{H} \rangle'$, $\mathbf{F}'$ at 100 keV to attempt extrapolations, but the temperature is clearly too low; indeed, the curve for $\langle \mathbf{H} \rangle'$ shows the onset of its angular limit at $T = 0$, and a close inspection of the curve for $\mathbf{F}'$ at the same temperature, $T = 100$ keV, detects "angular trends" as well. Hence, we shall use $T = 150$ keV for the calculation of $\mathbf{F}'$, and $T = 300$ keV for $\langle \mathbf{H} \rangle'$, as a compromise to obtain much less angular curves. As an additional precaution, we shall now use only the eight nuclei from ^{136}Sm to ^{143}Sm for the calculation of thermodynamical functions; we remove ^{135}Sm because of its lack of known excited states and ^{144}Sm because of shell closure effects. The difference, $\langle \mathbf{H} \rangle'_{300} - \mathbf{F}'_{150}$, is then plotted in Fig. 8.

The width of the band defined by $\langle \mathbf{H} \rangle'_{300}$ and $\mathbf{F}'_{150}$ as functions of $\langle \mathbf{A} \rangle'$ can be estimated from Fig. 8 to be ~ 800 keV. Smaller values at both ends are obviously misleading, because they represent the edge effects of the truncation of the data base, where the chemical potential is large with both signs.

Predictions might, thus, be listed with a ± 400 keV error. For a somewhat crude analytical continuation below ^{136}Sm, we make a least square fit by a cubic polynomial between ^{137}Sm and ^{142}Sm. Voluntarily, the fit does not

take into account the functions $\langle \mathbf{H} \rangle'_{300}$ and $\mathbf{F}'_{150}$ in the interval between ^{136}Sm and ^{137}Sm and in that between ^{142}Sm and ^{143}Sm, because we want to avoid the edge effects observed in Fig. 8. We accept an order 3 for the polynomials rather than the simpler order, 2, because we want to take into account a skewness of the plots of $\langle \mathbf{H} \rangle'$ and $\mathbf{F}'$. We verified that, despite such an odd order, such fitted polynomials still induce concavity in a large enough interval. The polynomial fitting $\langle \mathbf{H} \rangle'_{300}$ reads,

$$\mathcal{P}_H(\langle \mathbf{A} \rangle') \simeq -8.0\ (\langle \mathbf{A} \rangle' - 150.1)\ (\langle \mathbf{A} \rangle' - 141.1)\ (\langle \mathbf{A} \rangle' - 137.4), \tag{16}$$

and that fitting $\mathbf{F}'_{150}$ reads,

$$\mathcal{P}_F(\langle \mathbf{A} \rangle') \simeq -7.0\ (\langle \mathbf{A} \rangle' - 153.1)\ (\langle \mathbf{A} \rangle' - 142.9)\ (\langle \mathbf{A} \rangle' - 136.2). \tag{17}$$

The results are shown in Fig. 9, where the full curves represent the thermodynamical functions, as estimated numerically, and the dashed curves represent their polynomial fits, extrapolated.

It is seen that such polynomial approximations for $\langle \mathbf{H} \rangle'$ and $\mathbf{F}'$ define a "crescent" rather than a band, see Fig. 9. The method, therefore, has obviously a limited validity domain, so long as a better extrapolation scheme is not found. As seen from Fig. 9, "predictions" for ^{135}Sm and ^{134}Sm will be reasonable, but it seems more risky to use this method below ^{134}Sm. It is clear that the difficulty is due to the absence of known excited states for isotopes lighter than ^{136}Sm, making it impossible to estimate the thermodynamical functions below ^{136}Sm accurately enough.

Many prediction schemes can be provided by this method. For instance, the formula,

$$E_{pred}(A) = \frac{1}{2}\left[\mathcal{P}_H(A) + \mathcal{P}_F(A)\right] - 10000 \times A + 245000 - 1250 \times Mod[A+1,2] - 36 \times (A-139)^2, \tag{18}$$

takes the middle between the presumed upper bound, $\mathcal{P}_H(A)$, and the presumed lower bound, $\mathcal{P}_F(A)$; simultaneously, and necessarily, it inverts Eq. (15). The results for ^{133}Sm, ^{134}Sm, ^{135}Sm, and ^{144}Sm read, respectively, $\{-1081622, -1094280, -1104086, -1196422\}$, to be compared with the values taken from the mass tables, $E_A = \{-1082088, -1094512, -1103976, -1195736\}$. Hence the corresponding errors are, $E_{pred}(A) - E_A = \{466, 232, -110, -686\}$, to be compared with those from ^{137}Sm to ^{142}Sm, $\{-31, -8, 98, 25, -59, -35\}$ and those, $\{-79, -44\}$, for the two nuclei, ^{136}Sm and ^{143}Sm, that were excluded from our least square fit but contributed to the thermodynamical estimates. As expected from Fig. 9, such results for ^{134}Sm and ^{135}Sm are quite satisfactory; they lie very much inside the estimated error bar, ~ 400 keV. Somewhat unexpectedly, a tolerable result is found for ^{133}Sm. But, again as expected, if only from Fig. 9, a large error is found for ^{144}Sm.

Another formula,

$$E_{low}(A) = \mathcal{P}_F(A) - 10000 \times A + 245000 - 1250 \times Mod[A+1,2] - 36 \times (A-139)^2, \tag{19}$$

obviously gives candidate lower bounds. For ^{133}Sm, ^{134}Sm and ^{135}Sm, it generates the following errors, $E_{low}(A) - E_A = \{230, -38, -415\}$, with a serious failure for ^{133}Sm. But, if one does not trust such a formula beyond, say, one unit of mass below ^{135}Sm, another formula,

$$E_{tang}(A) = \mathcal{P}_F(134) + (A-134) \times \left.\frac{d\mathcal{P}_F}{dA}\right|_{A=134} - 10000 \times A + 245000 - 1250 \times Mod[A+1,2] - 36 \times (A-139)^2, \tag{20}$$

uses concavity and the derivative, $d\mathcal{P}_F/dA|_{A=134} \simeq -1619$, to predict lower bounds. With $\mathcal{P}_F(134) \simeq 2600$, the errors for ^{133}Sm, ^{134}Sm and ^{135}Sm become, $\{11, -38, -620\}$. As should be, the first and third numbers are smaller than those obtained from Eq. (19) and the second number is unchanged. More important, the first number, with still the wrong sign for an expected lower bound, is now so small that the "prediction" is excellent if it is not a fortunate coincidence. It should be kept in mind that our experimental data are anyhow accurate only within tens of keV.

In turn, the formula,

$$E_{up}(A) = \mathcal{P}_H(A) - 10000 \times A + 245000 - 1250 \times Mod[A+1,2] - 36 \times (A-139)^2, \tag{21}$$

is assumed to yield upper bounds. Then concavity states that the further formula,

$$E_{high}(A) = \frac{1}{2}\left[\mathcal{P}_H(A-1) + \mathcal{P}_H(A+1)\right] - 10000 \times A + 245000 - 1250 \times Mod[A+1,2] - 36 \times (A-139)^2, \tag{22}$$

yields higher upper bounds. For ^{133}Sm, ^{134}Sm and ^{135}Sm again, the respective errors read $\{702, 502, 195\}$ and $\{939, 715, 384\}$. The second set shows, as expected, larger errors than the first one.

This section, which uses Sm isotope data, has thus completely confirmed the theorems and properties, tested in the previous section with Sn isotope data. A limit to the validity of the method has been found, however: experimental

data for ^{133}Sm, ^{134}Sm and ^{135}Sm can be confirmed by this theory, but, because of a very severe lack of excited state data below ^{136}Sm, we find it unreasonable to extend the present "thermodynamical" theory all the way to ^{128}Sm, and even less reasonable to use it for predicting Sm isotopes lighter than ^{128}Sm. This does not prevent us, as an extension of the right part of Fig. 6, from attempting a polynomial fit for ground-state energies from, say, ^{135}Sm to ^{128}Sm and extrapolating for lighter nuclei. But the only "thermodynamical" aspect of such an extrapolation from just ground-state energies would be to retain the same error bar as that obtained from Fig. 8.

V. SUMMARY, DISCUSSION AND CONCLUSION

We first recalled [1] how a table of ground-state energies for a sequence of isotopes can be converted into a concave pattern. This involved simple manipulations: for instance an explicit term, accounting for pairing in even nuclei, can be subtracted from the bindings. Similar arguments leading to concavity are obviously possible for isotones as well, and furthermore for any other sequence of neighboring nuclei in any direction across the table of known nuclei. Once this empirical tuning has been implemented, linear or polynomial extra- and interpolations of the concave pattern may provide surprisingly accurate estimates of, or bounds for, binding energies. The terms which were added to induce concavity are subtracted *in fine*, naturally.

This work defined a more ambitious extra- and interpolation scheme, involving thermodynamical functions from a grand canonical ensemble, because such functions may have rigorous concavity properties. A few theorems are available, indeed. For instance, the free energy is a concave function of the average particle number. It is also a decreasing function of the temperature. We also found "quasi-theorems", more precisely strong numerical evidences, concerning the average energy. For instance, this average energy seems to be, except for minor accidents, a concave function of the average particle number.

For every given, finite temperature, we found that the average energy and the free energy, as functions of the average particle number, give upper and lower bounds, respectively, for the concave envelope of the ground-state energies. When the temperature vanishes, both bounds converge to the exact results.

A difficulty remains for extrapolations at this vanishing temperature, however: the analyticity of such thermodynamical functions is lost, because their limit is only piecewise continuous. It is, therefore, necessary to retain a minimum temperature if one wants to obtain practical extrapolations for the prediction of exotic nuclei. This is because a minimum amount of particle number fluctuation is obviously necessary to justify the conversion of particle number, an initially discrete quantity, into a continuous variable.

We, therefore, implemented numerical estimates of several thermodynamical functions at moderate temperatures, a few hundred keV at most. This yields a first result, namely a "band", enclosing ground-state energies between the average energy and the free energy. The width of the band defines an error bar which can be definitely trusted when extrapolations are made.

A difficulty arises, however, because of an insufficient number of excited states; these, obviously, are missing at both ends of any sequence of isotopes. More than often, only the ground-state energy is known for such neutron rich or neutron poor nuclei. The calculation of the average and free energies is thus possible only in an interval smaller than the interval of masses where ground states are known. Two tactics are then available, namely i) an extrapolation of the sequence of ground-state energies alone and ii) an extrapolation of the thermodynamical functions, starting from a smaller interval.

The first approach was the subject of our previous work [1], and the present work makes it more reliable because of the derivation of an error bar in this paper. The present work tested the second tactic, with some success. But a limitation was found: because of the lack of known excited states, edge effects are present in the calculation of thermodynamical functions and, therefore, it is better to restrict polynomial fits to even a slightly smaller mass interval. Then, extrapolations by means of such polynomials seem to be reliable within only two, at most three mass units towards drip lines.

It is clear that our polynomial extrapolations, while useful, do not take enough into account analytical properties which could be derived from the simplicity of an Hamiltonian of the form, $\mathbf{H} = \sum_i t_i + \sum_{i>j} v_{ij}$, and further analytical properties of thermodynamical functions such as $\mathcal{Z} = \mathrm{Tr}\exp[\beta(\mu\mathbf{A} - \mathbf{H})]$, Eq. (1). Semi-classical approximations, for instance, are likely to improve this method, when extrapolations are implemented. This is in our agenda.

In any case, we can make the strong conclusion that the combination of concavity and extrapolations of thermodynamical functions gives a systematic set of upper and lower bounds for the prediction of ground-state energies.

Acknowledgments: We thank I. Allison for helpful discussions and assistance with the management of the data sets. It is a pleasure for B. R. B. and B. G. G. to thank TRIUMF, Vancouver, B. C., Canada, for its hospitality, where part of this work was done. The Natural Science and Engineering Research Council of Canada is thanked for financial support. TRIUMF receives federal funding via a contribution agreement through the National Research Council

of Canada. B. R. B. also thanks Service de Physique Théorique, Saclay, France, for its hospitality, where another part of this work was carried out, and the Gesellschaft für Schwerionenforschung (GSI), Darmstadt, Germany, for its hospitality during the preparation of this manuscript, and acknowledges partial support from NSF grant PHY0555396 and from the Alexander von Humboldt Stiftung.

[1] B.R. Barrett, B.G. Giraud, B.K. Jennings and N.P. Toberg, arXiv:nucl-th/0707.4096, submitted to Phys. Rev. **C**
[2] G. Audi and A. H. Wapstra, Nucl. Phys. **A595**, 409 (1995).
[3] G. Audi, O. Bersillon, J. Blachot and A. H. Wapstra, Nucl. Phys.**A 624**, 1 (1997).
[4] P. Ekström, Nuclear Structure and Decay Data, http://nucleardata.nuclear.lu.se/database/masses/
[5] G. Audi, A.H. Wapstra and C. Thibault, Nucl. Phys. **A 729**, 337 (2003)
[6] *Table of Isotopes*, Firestone, Shirley, Baglin, Chu, Zipkin eds, Wiley

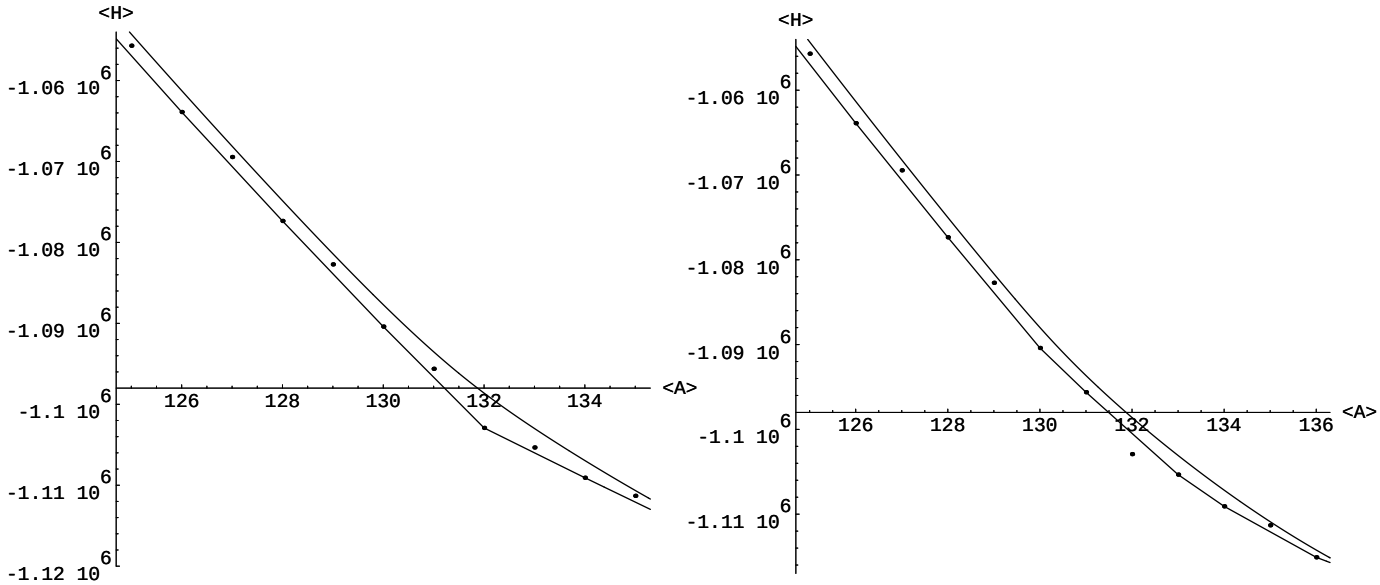

FIG. 1: Function $\langle \mathbf{H} \rangle (\langle \mathbf{A} \rangle)$ from bare data. Left, including ^{132}Sn. Right, without ^{132}Sn. Lower curves, $T = 20$ keV. Upper ones, $T = 2$ MeV. Note the failure of the low temperature curves at reproducing ground-state energies of odd nuclei.

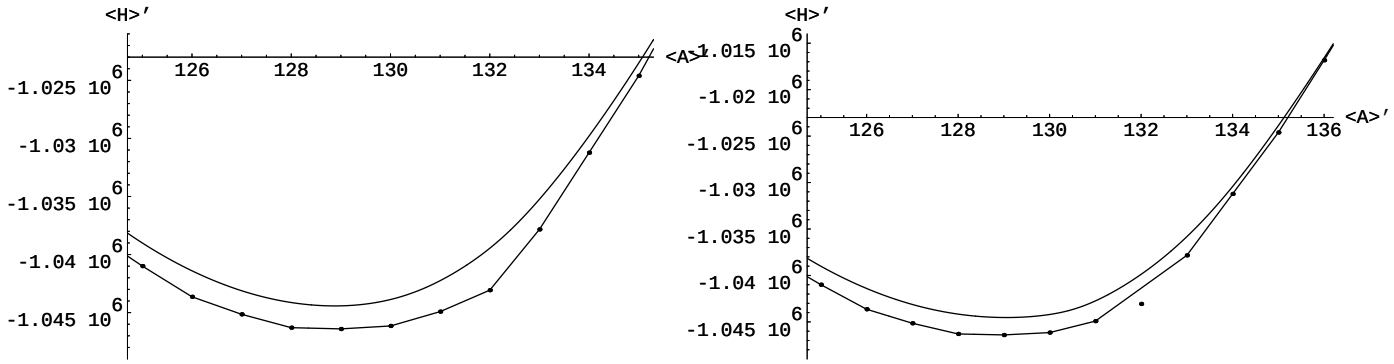

FIG. 2: Concave data $\langle \mathbf{H} \rangle'(\langle \mathbf{A} \rangle')$. Left, with ^{132}Sn. Right, without ^{132}Sn. Lower curves, $T = 20$ keV. Upper ones, $T = 2$ MeV. In contrast with Fig. 1, the lower curves reproduce the ground-state energies of both odd and even contributor nuclei.

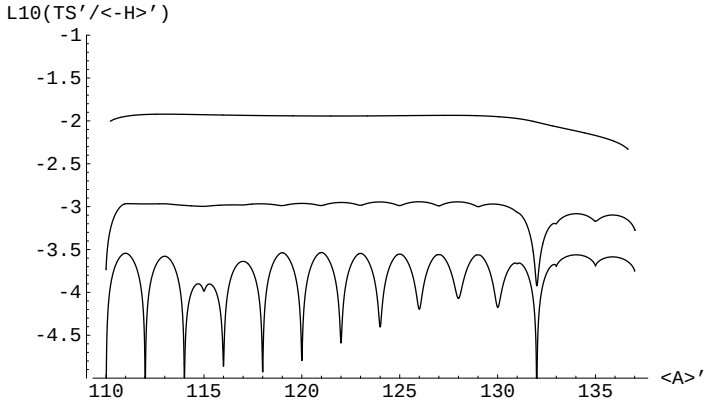

FIG. 3: Decimal log plots of $|T\,S'/\langle \mathbf{H} \rangle'|(\langle \mathbf{A} \rangle')$; upper curve, $T = 2$ MeV; intermediate one, $T = 300$ keV; lower one, 100 keV.

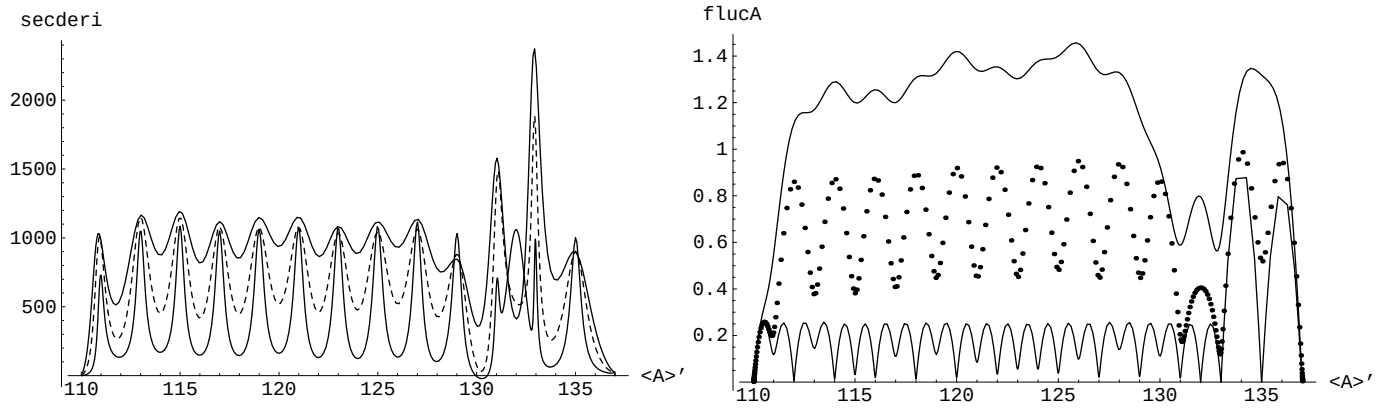

FIG. 4: Left, behavior of $\left(\langle \mathbf{A}^2\rangle' - \langle \mathbf{A}\rangle'^2\right) \partial^2\langle \mathbf{H}\rangle'/\partial\langle \mathbf{A}\rangle'^2$; upper full line, $T = 1$ MeV; dashed curve $T = 750$ keV; lower full line, 500 keV. Right, behavior of $\langle \mathbf{A}^2\rangle' - \langle \mathbf{A}\rangle'^2$; upper curve, $T = 1$ MeV; dots, $T = 500$ keV; lower curve, 100 keV.

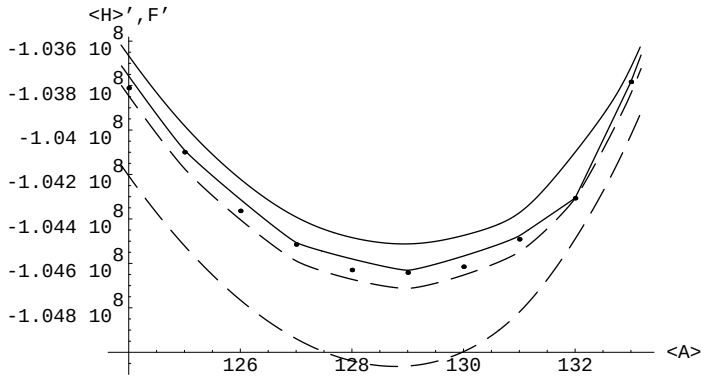

FIG. 5: Upper full curve, average energy $\langle \mathbf{H}\rangle'$ for $T = 1$ MeV, lower full one, same for $T = 250$ keV. Upper dashed curve, free energy $\mathbf{F}'$ for $T = 250$ keV, lower dashed one, same for $T = 1$ MeV.

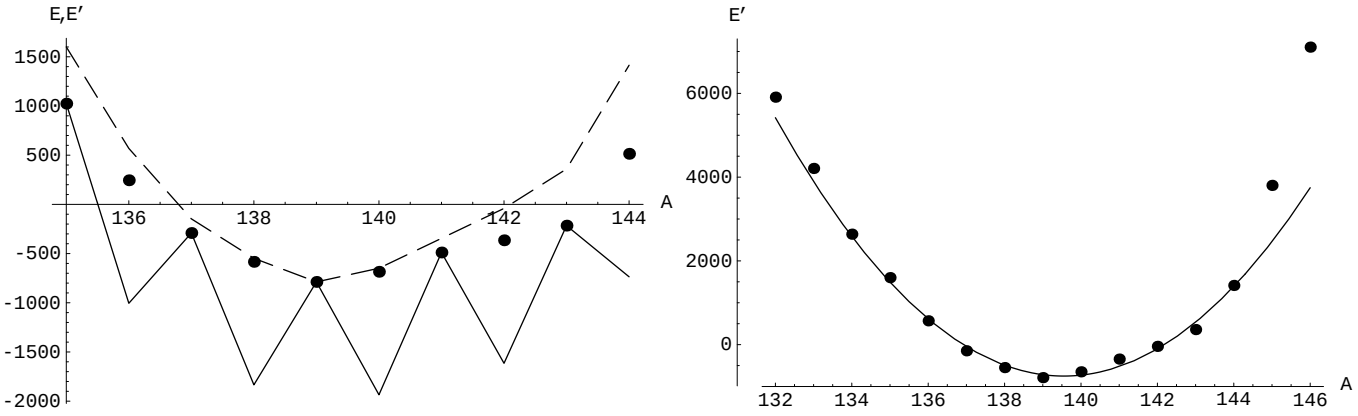

FIG. 6: Left: the full line joins Sm energies $E_A + 10000 \times A - 245000$; the dots show the result of the pairing correction; the long dashed line connects tuned, "concave energies" E'_A. Right: dots, same tuned energies, from ^{132}Sm to ^{146}Sm; full line, least square fit by degree 2 polynomial between ^{135}Sm and ^{144}Sm only.

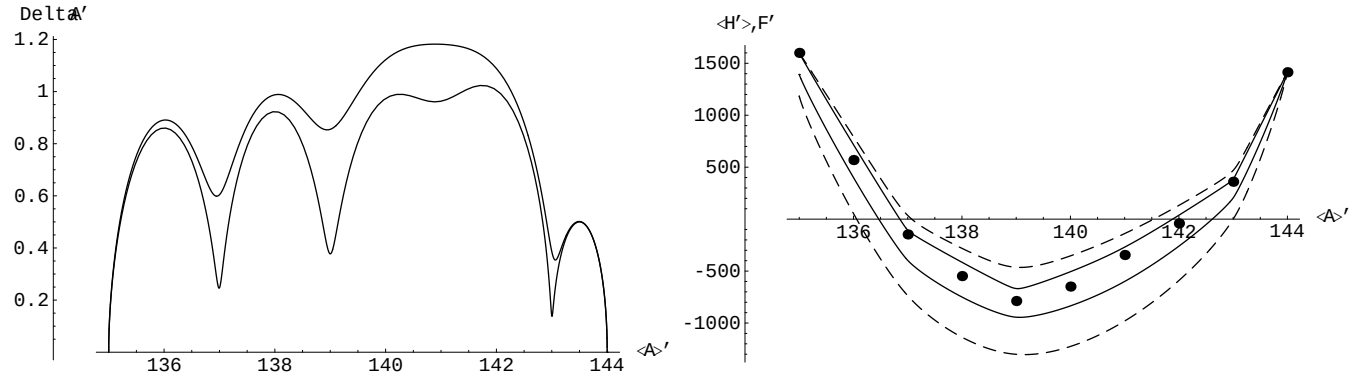

FIG. 7: Left: Sm particle number fluctuation at 200 (upper curve) and 100 keV (lower curve). Right: dots, Sm ground-state tuned energies; upper two curves, $\langle \mathbf{H} \rangle'$; lower two curves, $\mathbf{F}'$; dashed curves, $T = 200$ keV, full ones, $T = 100$ keV.

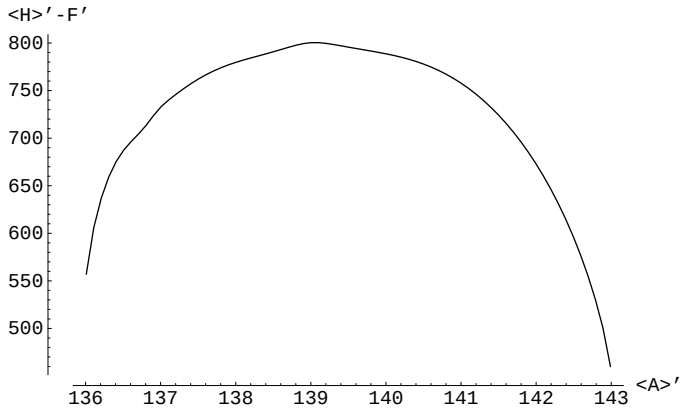

FIG. 8: Estimation of an error bar from the difference, $\langle \mathbf{H} \rangle'_{300} - \mathbf{F}'_{150}$, as a function of $\langle \mathbf{A} \rangle'$.

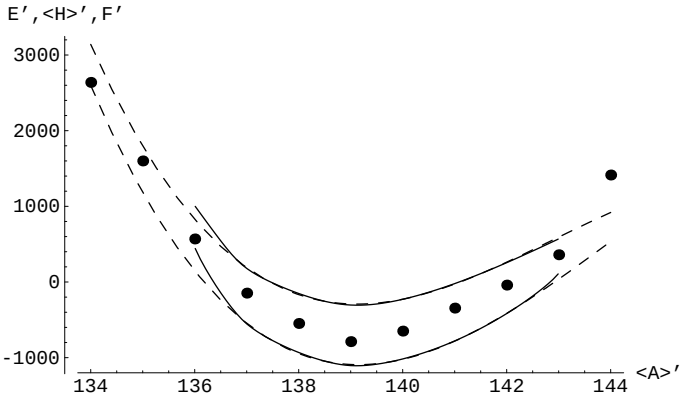

FIG. 9: Full curves: $\langle \mathbf{H} \rangle'_{300}$ (upper) and $\mathbf{F}'_{150}$ (lower), calculated with eight spectra, from ^{136}Sm to ^{143}Sm. Dashed curves: cubic polynomials obtained by least square fits between ^{137}Sm and ^{142}Sm. Dots: actual values E'_A.